A Hydrodynamic Lake Model Coupled with a Three-Dimensional Dynamic Visualization Method

Xianyong Gu
Tongji University College of Environmental Science and Engineering
Zhenliang Liao (zl_liao@tongji.edu.cn)
Tongji University College of Environmental Science and Engineering https://orcid.org/0000-0002-1267-7460
Guozheng Zhi
Shanghai Urban Water Resources Development and Utilization National Engineering Center Co., Ltd.
Wenchong Tian
Tongji University College of Environmental Science and Engineering
Jiaqiang Xie
Yangtze Ecology and Environment Co., Ltd.

Research Article

Keywords: Three-dimensional dynamic visualization, Lake, Hydrodynamic model, Integration

Posted Date: July 6th, 2021

DOI: https://doi.org/10.21203/rs.3.rs-540382/v1

A hydrodynamic lake model coupled with a three-dimensional dynamic visualization method

Xianyong Gu[1], Zhenliang Liao[1,], Guozheng Zhi[2], Wenchong Tian[1], Jiaqiang Xie[3],*

1. College of Environmental Science and Engineering, Tongji University, 200092 Shanghai, China

2. Shanghai Urban Water Resources Development and Utilization National Engineering Center Co., Ltd., 200082 Shanghai, China

3. Yangtze Ecology and Environment Co., Ltd., 430077 Wuhan, China

*Corresponding author(s):

Tel.: +86 (0)21 65981650; fax: +86 (0)21 65986313. (Z. Liao)

E-mail address(es):

zl_liao@tongji.edu.cn (Z. Liao)

Acknowledgements

This study is financially supported by Major Science and Technology Program for Water Pollution Control and Treatment (Grant No. 2018ZX07208006 and Grant No. 2017ZX07603001). The authors also thank Academic Capability Improvement Plan of Tongji University, and National Geographic Resource Science SubCenter, National Earth System Science Data Center, National Science & Technology Infrastructure of China (http://gre.geodata.cn).

Abstract

The hydrodynamic lake model is an important tool for lake management and decision-making. When model results are analyzed by the traditional analysis methods, the multi-source heterogeneous data are not expressed systematically and intuitively, which leads to the inability to extract useful information efficiently. In order to solve the above problems, a three-dimensional dynamic visualization analysis method of the hydrodynamic lake model (3DV-HLM) is proposed by coupling the hydrodynamic lake model and the three-dimensional dynamic visualization technology. Chaohu Lake is taken as an example to verify the feasibility of the method. 13 working conditions are set up and the simulated water flows changing with space and time are analyzed and compared by the 3DV-HLM method. Results show that the 3DV-HLM method proposed in this study is more systematic and effective in the expression of multi-source heterogeneous information than the traditional analysis methods. It is easier to discover rules and obtain useful information from huge data set by the 3DV-HLM method. Besides, the intuitive display of the model results by the 3DV-HLM method is close to the real environment, which can enhance the understanding of the hydrodynamic characteristics of the lake by the water environment managers.

Keywords: Three-dimensional dynamic visualization; Lake; Hydrodynamic model; Integration

1. Introduction

The hydrodynamic lake model plays an important role in the lake research, and it is an effective tool for simulating and predicting water flows of the lake under specific working conditions. On the one hand, the hydrodynamic model can reveal hydrodynamic characteristics of the lake including water levels and water flows. On the other hand, the hydrodynamic model provides important hydrodynamic background conditions for the establishment of the water quality model (Yadav and

Zhang 2020; Zhao et al. 2020; Wang et al. 2019; Qi et al. 2019; Wurjanto and Ajiwibowo 2019).

However, the traditional analysis methods of the hydrodynamic lake model results need to be improved in coupling of multi-source heterogeneous data, extraction of useful information, and intuitive expression of the data (Cao and Hou 2008; Zhang et al. 2008; Wu and Tsanis 1995). The hydrodynamic lake model runs and generates large amounts of three-dimensional data that change with time and space, and the analysis of model results involves real three-dimensional geographic environment such as ground features and terrain. The two-dimensional charts and tables which are often used can only analyze part of the three-dimensional data. Therefore, the expression of information is not systematic and effective enough (Pang et al. 2015; Wang et al. 2016). As for the analysis of multi-source data, the two-dimensional limitation of the traditional method leads to difficulty in extracting valuable information and finding rules (Zhang et al. 2020; Zhang et al. 2019; Wang et al. 2019). Besides, due to poor human-computer interaction, the traditional analysis methods cannot provide real three-dimensional water flow state from various perspectives, and this leads to nonintuitive expression of information. Therefore, it is a major challenge to use spatial information effectively, couple and analyze multi-source heterogeneous data, and improve the visualization of model results so that the efficiency of decision making in the lake management can be improved.

In recent years, with the rapid improvement of computer processing capabilities, it is possible to process large amounts of multi-source data. The three-dimensional visualization technology has been developed and is widely used in research fields such as medical diagnosis, meteorological simulation, and geological exploration (Li et al. 2012; Wang et al. 2013; Saravanavel et al. 2020; Rodriguezgonzalvez et al. 2018; Tame et al. 2013). In the field of water environment, the application of three-dimensional visualization mainly focuses on the groundwater and river channels (Kolditz et

al. 2019; Zhi et al. 2019; Li et al. 2021). As for lakes, some scholars researched the three-dimensional visualization of measured data. These researches are not combined with the hydrodynamic lake models, so they do not have the function of simulating and predicting lake water flows, and this restricts the analysis and decision-making functions of the lake management (Robinson et al. 2020).

In view of the above-mentioned shortcomings of the traditional analysis methods, this research studies the integration of the hydrodynamic lake model and the three-dimensional dynamic visualization technology. The purpose of this paper is to construct a three-dimensional dynamic visualization analysis method of the hydrodynamic lake model (3DV-HLM), and Chaohu Lake in China is selected as a case to verify the method. The second part of this article mainly introduces the research data sources, the integration method of the hydrodynamic model and the three-dimensional visualization theory. The third part gives the flow field results at different running times under the typical working condition and the visual comparison results of flow fields under different working conditions. The fourth part compares and discusses the traditional analysis method and the 3DV-HLM method. The last part gives the conclusion of the article.

2. Data and methods

The theoretical methods in this study mainly include the construction of hydrodynamic lake model, the development of data interface, and the construction of three-dimensional dynamic visualization method. 13 working conditions are set up according to different initial water levels, wind directions, wind speeds, and river flows. A multi-scheme synchronous comparison method is used to analyze the hydrodynamic characteristics of Chaohu Lake. The theoretical framework of the research is shown in Fig. 1.

2.1 Study area

Chaohu Lake is located in Anhui Province, China. It is a shallow lake, with an average water depth of 3.06m. The average water temperature of Chaohu Lake is about 16.9℃, and the average water level of Chaohu Lake is 8.33 m. The east wind has the highest frequency in Chaohu Lake, and the annual average wind speed of Mushan Station on the lake is 2.7 m/s. There are mainly 7 rivers connected with the lake, and the river discharges flowing into the lake vary greatly in different typical periods (i.e., dry season, normal season, and wet season). Water in Chaohu Lake can flow into the Yuxi River through the Chaohu Floodgate. The location of Chaohu Lake and the inflowing rivers are shown in Fig.2.

2.2 Model description

2.2.1 Coordinates and equations

The orthogonal curvilinear co-ordinate is used in the horizontal direction, and the σ co-ordinate system is used in the vertical direction. The σ co-ordinate system is defined as:

$$\sigma = \frac{z-\zeta}{d+\zeta} = \frac{z-\zeta}{H}, \tag{1}$$

where z is the vertical co-ordinate in physical space, m; ζ is the free surface elevation above the reference plane, m; d is the depth below the reference plane, m; H is the total water depth, given by $H = d + \zeta$.

The Navier-Stokes equations for an incompressible fluid under the shallow water and the Boussinesq assumptions are used by the hydrodynamic lake model. The depth-averaged continuity equation is given by:

$$\frac{\partial \zeta}{\partial t} + \frac{1}{\sqrt{G_{\xi\xi}}\sqrt{G_{\eta\eta}}}\frac{\partial[(d+\zeta)u\sqrt{G_{\eta\eta}}]}{\partial \xi} + \frac{1}{\sqrt{G_{\xi\xi}}\sqrt{G_{\eta\eta}}}\frac{\partial[(d+\zeta)v\sqrt{G_{\xi\xi}}]}{\partial \eta} = Q, \tag{2}$$

where Q is the contributions per unit area due to the discharge or withdrawal of water,

precipitation and evaporation; u and v are the depth averaged velocities of ξ- and η-direction respectively.

The momentum equations in ξ- and η-direction are given by:

$$\frac{\partial u}{\partial t}+\frac{u}{\sqrt{G_{\xi\xi}}}\frac{\partial u}{\partial \xi}+\frac{u}{\sqrt{G_{\eta\eta}}}\frac{\partial u}{\partial \eta}+\frac{\omega}{d+\zeta}\frac{\partial u}{\partial \sigma}+\frac{uv}{\sqrt{G_{\xi\xi}}\sqrt{G_{\eta\eta}}}\frac{\partial\sqrt{G_{\eta\eta}}}{\partial \eta}-\frac{v^2}{\sqrt{G_{\xi\xi}}\sqrt{G_{\eta\eta}}}\frac{\partial\sqrt{G_{\eta\eta}}}{\partial \eta}-fv=-\frac{1}{\rho_0\sqrt{G_{\xi\xi}}}P_\xi+F_\xi+\frac{1}{(d+\zeta)^2}\frac{\partial}{\partial\sigma}\left(v_v\frac{\partial u}{\partial\sigma}\right)+M_\xi, \quad (3)$$

$$\frac{\partial v}{\partial t}+\frac{u}{\sqrt{G_{\xi\xi}}}\frac{\partial v}{\partial \xi}+\frac{v}{\sqrt{G_{\eta\eta}}}\frac{\partial v}{\partial \eta}+\frac{\omega}{d+\zeta}\frac{\partial v}{\partial \sigma}+\frac{uv}{\sqrt{G_{\xi\xi}}\sqrt{G_{\eta\eta}}}\frac{\partial\sqrt{G_{\eta\eta}}}{\partial \xi}-\frac{u^2}{\sqrt{G_{\xi\xi}}\sqrt{G_{\eta\eta}}}\frac{\partial\sqrt{G_{\xi\xi}}}{\partial \eta}+fu=-\frac{1}{\rho_0\sqrt{G_{\eta\eta}}}P_\eta+F_\eta+\frac{1}{(d+\zeta)^2}\frac{\partial}{\partial\sigma}\left(v_v\frac{\partial v}{\partial\sigma}\right)+M_\eta, \quad (4)$$

where ω is the velocity of σ-direction, and ω is computed from the continuity equation:

$$\frac{\partial\xi}{\partial t}+\frac{1}{\sqrt{G_{\xi\xi}}\sqrt{G_{\eta\eta}}}\frac{\partial[(d+\zeta)u\sqrt{G_{\eta\eta}}]}{\partial\xi}+\frac{1}{\sqrt{G_{\xi\xi}}\sqrt{G_{\eta\eta}}}\frac{\partial[(d+\zeta)v\sqrt{G_{\xi\xi}}]}{\partial\eta}+\frac{\partial\omega}{\partial\sigma}=H(q_{in}-q_{out}), \quad (5)$$

where $G_{\xi\xi}$ and $G_{\eta\eta}$ are the conversion coefficients of the coordinate system; F_ξ and F_η represent the unbalance of horizontal Reynold's stresses; M_ξ and M_η represent the contributions due to external sources or sinks of momentum; ρ_0 is the water density; v_v is the vertical eddy viscosity coefficient; f is the Coriolis coefficient; P_ξ and P_η represent the pressure gradients.

5 calculated layers are set in vertical direction of the model. The Alternating Direction Implicit (ADI) method is used to discretize and solve the equations. In order to have a stable calculation, the time step should satisfy the following condition:

$$2\Delta t\sqrt{gH}\sqrt{\frac{1}{\Delta x^2}+\frac{1}{\Delta y^2}}<1 \quad (6)$$

where v_H is the horizontal eddy viscosity coefficient; $\Delta x=\sqrt{G_{\xi\xi}}$ and $\Delta y=\sqrt{G_{\eta\eta}}$ are the minimum grid size of the calculation area in the x direction and y direction.

2.2.2 Model calibration and validation

The model is calibrated and verified by using Mean Relative Error (MRE). Results in Table 1 show that the model accuracy is high enough to meet the application requirements. The parameters after

calibration and verification are as follows: the manning roughness coefficient is 0.02; the wind drag coefficient is 0.026; horizontal and vertical diffusion coefficients are 10 m^2/s and 4 cm^2/s respectively; horizontal and vertical eddy viscosity coefficients are 10m^2/s and 4 cm^2/s respectively. The time step of model is set to 1 min.

Table 1 The velocity errors of model calibration and verification

Parameters	Model calibration	Model verification
Water level	1.39%	1.68%
Velocity magnitude	17.61%	20.10%

2.3 Data interface

Different sources, types and structures of data are involved in the analysis of hydrodynamic lake model. The data in this study mainly include structured data and unstructured data. The structured data mainly include the size, direction, color of three-dimensional flow arrows, attribute data, and modeling data. The unstructured data mainly include the terrain, remote sensing images, pictures, textures, materials, and three-dimensional model files.

In the study, a file database is used to store the data. According to the data structure and the functional requirements, a data interface is designed and established to transform the modeling data into the attribute data that can be recognized by the three-dimensional visualization system. Each visual object has a unique ID, through which the data in the database can connect with the visual object so that the attributes of the visual objects can change dynamically. The principle of the data interface is shown in Fig. 3.

The mouse operations are judged by the code. The mouse attributes are converted into distance or angle according to a certain mapping relationship, and then the converted data are transferred to the attributes of the field camera. Finally, the multi-scheme interactive operations of the three-dimensional scene are realized, including the translation, zoom and rotation of the scene.

2.4 Three-dimensional visualization method

According to the characteristics of the multi-source data and visual functional requirements, a three-dimensional dynamic visualization method applicable for the hydrodynamic lake model is established. The method mainly includes the construction of the geographic environment, the color conversion method, and the arrow transformation method of the flow field.

2.4.1 Construction of the geographic environment

The construction of the three-dimensional scene affects the system authenticity, and it is also the basis of coupled hydrodynamic lake model and the analysis of multi-source data. The elevation data H of the Digital Elevation Model (DEM) is used to express the terrain height, and two-dimensional space (X, Y) is extended to three-dimensional space (X, Y, Z). The mathematical expression is as follows:

$$H = f(X,\ Y) \tag{7}$$

The remote sensing image data are superimposed on the terrain elevation data to depict the texture images and enhance the realism of terrain rendering. The direct linear transformation method of the texture mapping is used to determine the texture attribute at any visible point P on the ground according to the mapping relationship from two-dimensional texture space (U, V) to three-dimensional terrain space (X, Y, Z). Finally, the terrain file is created from the DEM. The schematic diagram of the three-dimensional terrain construction is shown in Fig. 4.

2.4.2 Color conversion method

The color conversion method is used to convert the data into corresponding colors. Firstly, the data are normalized to a range between 0 and 1. Then the data can be converted to the color space by

a mapping relationship. The specific conversion formulas of variable x and color components R(x), G(x), B(x) and are as follows:

$$R(x)=\begin{cases}1-5det, & 0\le det\le 0.2\\ 0, & 0.2<det\le 0.6\\ 5det-3, & 0.6<det\le 0.8\\ 5-5det, & 0.8<det\le 1\end{cases} \tag{8}$$

$$G(x)=\begin{cases}0, & 0\le det\le 0.2\\ 5det-1, & 0.2<det\le 0.4\\ 3-5det, & 0.4<det\le 0.6\\ 1, & 0.6<det\le 0.8\\ 5-5det, & 0.8<det\le 1\end{cases} \tag{9}$$

$$B(x)=\begin{cases}1, & 0\le det\le 0.4\\ 3-5det, & 0.4<det\le 0.6\\ 0, & 0.6<det\le 1\end{cases} \tag{10}$$

$$det=\frac{x-x_{min}}{x_{max}-x_{min}} \tag{11}$$

where x is the value at a certain location of the model result; x_{max} is the maximum value of x; x_{min} is the minimum value of x; det is the value after normalization. Then the variable x is mapped to the corresponding color. The color band is shown in Fig 5.

After that, the calculated color values are associated with the shader corresponding to the object material, then they are processed and rendered by the vertex shader. As time changes, the color attributes of the shader change through the code. Finally, the dynamic three-dimensional visualization effect of the model results can be realized.

2.4.3 Arrow transformation method

The three-dimensional arrow transformation method is used to visualize the dynamic water flow of the lake. The three-dimensional arrow direction expresses the flow direction, and the length and color of the arrow are modified to reflect the flow magnitude change. The designed and constructed three-dimensional arrow model is used as a prefab, and the prefab is instantiated in batches through

code. The initial position and direction of the arrow are set to the grid coordinate and the x-axis direction respectively. In order to realize the dynamic change of the three-dimensional flow arrow, the size and color of the arrow need to be specified. The velocity components of the hydrodynamic model simulation results are converted to the arrow direction and arrow magnitude according to the following transformation formulas:

$$L_v = k \cdot \sqrt{{v_x}^2 + {v_z}^2} \tag{12}$$

$$\theta_v = \begin{cases} \tan^{-1}\frac{v_z}{v_x}, & v_x > 0, v_z > 0 \\ \tan^{-1}\frac{v_z}{v_x} + \pi, & v_x < 0 \\ \tan^{-1}\frac{v_z}{v_x} + 2\pi, & v_x > 0, v_z < 0 \\ \frac{\pi}{2} & v_x = 0, v_z > 0 \\ \frac{3}{2}\pi & v_x = 0, v_z < 0 \end{cases} \tag{13}$$

Where v_x and v_z are the speeds in the x- and z- direction respectively, k is the scale factor of the arrow length, L_v is the length of the arrow model, θ_v is the angle between the arrow model direction and the positive direction of the x-axis.

In the three-dimensional scene, there are two coordinate systems, namely the global coordinates of the scene and the local coordinates of each object. The global coordinates and the local coordinates are the black arrows and the red arrows in Fig. 6 respectively. The calculated arrow length L_v and arrow pointing angle θ_v of each time step are assigned to the scale attribute and rotation attribute of the arrow object respectively. The color of the arrow model is used to express the flow magnitude based on the color conversion method.

2.5 Analyzing methods of schemes

According to the measurement data, the initial water levels of 7.50m, 8.33m, 9.16m and 12.50m are set to simulate the flow field of Chaohu Lake. Considering that the temperature has little effect on the hydrodynamic model, the temperature is set to the average value. In order to find the influence of wind direction on water flows, the east, southeast, northeast, and northwest winds that occur frequently are simulated. The wind speeds of 0.9m/s, 2.7m/s, 4.5m/s and 12m/s are set to find the influence of wind speed on water flows. In addition, the flow rates of the into-lake rivers are calculated to simulate the flow field of Chaohu Lake at the dry period, normal period, and wet period. Detailed simulation schemes are shown in Table 2, and scheme 2 is chosen as the typical working condition.

Table 2 The schemes of hydrodynamic simulation

No.	Initial water level	Wind direction	Wind speed	River flows	Water temperature
1	7.5	East	2.7	Multi-year average	16.9
2	8.33	East	2.7	Multi-year average	16.9
3	9.16	East	2.7	Multi-year average	16.9
4	12.5	East	2.7	Multi-year average	16.9
5	8.33	Northeast	2.7	Multi-year average	16.9
6	8.33	Southeast	2.7	Multi-year average	16.9
7	8.33	Northwest	2.7	Multi-year average	16.9
8	8.33	East	0.9	Multi-year average	16.9
9	8.33	East	4.5	Multi-year average	16.9
10	8.33	East	12	Multi-year average	16.9
11	8.33	East	2.7	Dry period	16.9
12	8.33	East	2.7	Normal period	16.9
13	8.33	East	2.7	Wet period	16.9

Considering that visualization of a single scheme cannot meet the analyzing requirement, a multi-scheme comparison method is used in this study. The simulation results of the hydrodynamic lake model under different schemes are respectively visualized by different scene cameras, and then the three-dimensional dynamic multi-scheme analysis can be realized intuitively to compare different schemes simultaneously. The scene cameras are controlled by the code to realize the multi-scheme interactive operation between the mouse and the three-dimensional scene, including the translation,

zooming and rotation of the scene.

3. Results

According to the schemes in section 2.5, the research results mainly include the three-dimensional visualized flow field at different times under the typical working condition, and the three-dimensional visualized stable flow field under different water levels, wind directions, wind speeds, and river discharges.

3.1 Typical operating condition

The lake water flow changes complicatedly and presents different flow patterns at different times. In order to find the changing rules of lake water flow at different times more intuitively, the 3DV-HLM method is used to describe the dynamic changes of the lake water flow. Scheme 2 is chosen as the typical working condition. The model simulation results after the model runs for 1h, 4h, 12h, 72h are shown in Fig. 7 a-d. The lower left and the lower right of each subfigure show the flow state of point M and point N respectively by operating the three-dimensional perspective of the scene camera. From Fig. 7, we can clearly see the overall changes of the lake flow field at each moment. After the model runs for 72h, the flow field of Chaohu Lake is stable, and the distribution difference of the flow direction in the vertical direction becomes smaller.

3.2 Flow fields under different initial water levels

In order to find the impact of different initial water levels on the lake water flows, the 3DV-HLM method is used to analyze the simulation results under different initial water levels. The model results become stable after the model has been running for 72h, and the stable flow field at this time is selected for analysis. The three-dimensional visualized results of the simulated flow fields with initial water

levels of 7.55m, 8.33m, 9.16m, and 12.5m are shown in Fig. 8 a-d. It can be clearly seen from the figure that the 3DV-HLM method has advantages in the expression of water flow results, and it is easier to find the difference and connection among the top water flows, middle water flows, and bottom water flows. As the initial water level increases, the velocity magnitude of the lake decreases. It can be seen from the close-range view of point M and point N in Fig. 8d that when the water level reaches 12.5m, the directions of point M and point N of the surface flow are quite different from that of the 4 layers below.

3.3 Flow fields under different wind directions

In order to find the impact of wind directions on the lake water flows, the 3DV-HLM method is used to analyze the simulated flow fields under different wind directions. The three-dimensional visualized flow fields after the model has been running for 72 hours under east wind, northeast wind, southeast wind, and northwest wind are shown in Fig. 9 a-d respectively. It can be seen from the figure that under different wind directions, the lake has different circulation patterns. It is easier to find the influence of topography on the flow state at a certain point by using the 3DV-HLM method to visualize the flow field.

3.4 Flow fields under different wind speeds

In order to find the impact of wind speeds on the lake water flows, the flow fields under different wind speeds are simulated and analyzed by the 3DV-HLM method. The east wind which has the highest frequency of occurrence is taken as an example. The three-dimensional visualized flow fields after the model has been running for 72 hours under wind speeds of 0.9m/s, 2.7m/s, 4.5m/s, and 12m/s are shown in Fig. 10 a-d. Overall, as the wind speed increases, the shape of the flow field is almost unchanged, and the flow velocity magnitude increases. It is easier to notice the small differences

among the layers of the flow field by using the 3DV-HLM method.

3.5 Flow fields under different river discharges

In order to find the impact of different river discharges flowing into the lake on the lake water flows, the flow fields under different river discharges are simulated and analyzed by the 3DV-HLM method. The three-dimensional visualized flow fields after the model has been running for 72 hours under the dry period, normal period, and wet period are shown in Fig. 11 a-c. From an overall point of view, the lake under different periods have similar flow field patterns. Only the flow velocity at the point near the river mouth is changed slightly by the river discharges.

4. Discussion

Based on the above results, this part analyzes and compares the traditional method and the 3DV-HLM method from the expression of multi-source information, the extraction of rules, and the effect of visualization. For the convenience of discussion, the flow field after the model has been running for 72 hours under the typical working condition is taken as an example. The comparison by the traditional analysis method and the 3DV-HLM method are shown in Fig. 12 a-g.

4.1 Presentation of information

Compared with the traditional analysis method, the 3DV-HLM method proposed in this study is more systematic and efficient in the expression of multi-source heterogeneous information.

When analyzing the results of the hydrodynamic lake model, the traditional two-dimensional analysis method mainly focuses on the local data (Ying et al. 2018; Nutz et al. 2015; Zhang et al. 2019). For example, some researchers analyze a certain layer or a local point of the flow field, as shown in Fig. 12a-d. Although the traditional analysis method can also show some water flow information to a

certain extent, it is not complete and efficient in the expression of information.

The traditional analysis method does not include the three-dimensional terrain, islands and other ground features. This limits the three-dimensional analysis of water flows, such as researching the impact of the lake's central Mushan Island and the lakeshore topography on the water flows. In addition, when the research object is a deep lake or reservoir, it needs to be divided into more calculated layers in the vertical direction. In this situation, the traditional analysis method can only list more two-dimensional charts like Fig 12a-c, which greatly reduces the expression efficiency of the flow information.

The 3DV-HLM method is more systematic and efficient in the expression of information. Corresponding to Fig. 12a-c of the traditional method, the 3DV-HLM method can show the simulation results of the entire flow field in 5 calculated layers simultaneously, as shown in Fig. 12e. Fig. 12f shows a partial enlarged view of the Lake, and Fig. 12g shows the three-dimensional flow information corresponding to the point in Fig. 12d. It can be clearly seen from the figure that compared with the traditional analysis method, the 3DV-HLM method not only fully expresses the water flow information of the model result, but also includes more information such as topography and island. The three-dimensional analysis becomes possible by the 3DV-HLM method.

In Fig. 10a-d, only one interface is needed to show the comparison results of the simulated flow field at all points simultaneously under different wind speeds. It can be seen from Fig. 10a-c that when the wind speed changes, only the surface water flow directions at points M and N change slightly. It can be seen from Fig. 10d that in the case of a maximum wind speed of 12m/s, the average flow magnitudes at points M and N vary greatly, but the vertical distribution of the flow direction is almost the same with that under small wind speeds. In addition, the viewpoint switching function is added to

the scene camera so that the view angle can be changed to the point of interest quickly by operating the mouse. Compared with the traditional method, the 3DV-HLM method presents more data by using fewer charts, and the presentation of the results is more in line with the real three-dimensional environment, which makes the expression of information more efficient.

4.2 Extraction of rules

Compared with the traditional analysis method, it is easier to capture useful information from huge data and discover potential regular rules by the 3DV-HLM method.

Due to the limitation of two dimensions, the traditional two-dimensional analysis method can only separate the flow field by layer to perform limited analysis on each layer. In this case, the continuity of the flow field in the three-dimensional space is ignored, and it is not conducive to finding details of the flow field. For example, in Fig. 12 b and c, although the water flow characteristics can be analyzed for each calculated layer, it is easy to draw the wrong conclusion that the flow fields in the middle layer and the bottom layer are the same. The subsistent small differences between the layers cannot be identified correctly.

In the analysis of the water flow of a certain point, the traditional analysis method can only analyze the vertical distribution of water velocity magnitude and direction separately (Ren et al. 2015), as shown in Fig. 12d. It is difficult for the researchers to understand the true velocity state of the point in the three-dimensional space, and it is also impossible to analyze the relationships between the flow at certain point and the surrounding water flows.

By using the 3DV-HLM method, it is easier to discover the rules of the water flows. Compared with Fig. 12a-c, from Fig 7a-d, the changing rule with the model running time of the three-dimensional lake flow field can be seen more clearly. For example, when the model started to run, the flow

directions of the top and the second layer (including point M and N) of the lake are the same with the wind direction, and the flow directions of the penultimate and bottom layer are opposite to the wind direction, which is a compensation flow. When the model runs for 4 hours, the flow directions at points M and N are stable. After that, the flow velocity magnitude increases slightly. When the model runs for 72 hours, the flow field is completely stable. At this time, two large circulations symmetrical about the center line are formed in the lake.

Compared with Fig. 12d, it is easier to find from Fig. 12g that the water flow direction has a slight changing angle along the water depth in the vertical direction under certain conditions. It can be seen from Fig. 8a-d that the vertical distribution difference of the water flow direction increases with the increase of the initial water level. In addition, it can be clearly seen from Fig. 8d that when the initial water level is higher, the angle formed by the surface flow direction and the flow directions of the lower four layers at point M and point N is larger. These details are easily ignored in previous studies.

It can be seen clearly from Fig. 9a-d and Fig. 12f that the wind directions have great effect on the circulation patterns of the lake. For example, under the influence of the northeast wind, the west lake forms a circulation with Mushan Island as the boundary, which is not conducive to the degradation of pollutants in the west lake. The middle lake and the east lake form two large circulations symmetrical about the center line. Under the influence of the southeast wind, the west lake and the middle lake form two large circulations symmetrical about the center line, while the east lake forms a circulation. Under the influence of the northwest wind, the circulation pattern of the lake is similar to that under the southeast wind, but the circulation direction is opposite.

After the flow field is stable, the circulation patterns of the five calculated layers have little difference, but the water flow direction at certain points changes along the water depth. For example,

under the east wind, northeast wind, northwest wind, the flow directions of point M and point N have gradual angle changes along the water depth. The rules above are not easy to find by the traditional two-dimensional analysis method. In addition, it can be seen from Figs 9a-d that the vertical distribution characteristics of the water flows in the center of the lake are more affected by the wind, while the vertical distribution characteristics of the water flows near the shore are more affected by the topography. Owing to the advantage that the 3DV-HLM method has one more dimension than the traditional analysis method and the 3DV-HLM method integrates more data such as terrain and ground features, it is more conducive to the discovery of potential rules of the water flow.

4.3 Visualization effect and lake management

The 3DV-HLM method makes the model results more intuitive, which can enhance the understanding of the hydrodynamic characteristics of the lake by the decision makers and improve the efficiency of the lake management.

The traditional two-dimensional analysis methods often use two-dimensional charts to express the model results, which do not conform to the real three-dimensional water flow, so the visualization effect is poor. For example, as shown in Fig. 12a-d, the researchers cannot observe the lake flow field from multiple perspectives, and it is difficult to analyze the flow field in an intuitive way. In addition, due to the limitations of two dimensions, the decision makers cannot interact with research objects, which is not conducive to the management of the lake.

The three-dimensional lake system constructed in this research is closer to the real environment, so that it is easier for the researchers and decision makers to have an objective understanding of the real flow field. By using the 3DV-HLM method, the researchers and decision makers can roam in the three-dimensional scene, and the interactive analysis of the simulated lake flow field from multiple

perspectives become possible. For example, in Fig. 12e-g, the zooming, translation and rotation of the visual field can be realized only by operating the mouse.

It can be found from Fig. 11a-c that the river discharges flowing into the lake have a small impact on the lake circulation pattern. By operating the mouse and moving the scene camera to points M and N, it can be found that the impact of the river discharges on the velocity magnitude of point N is greater than that of point M. This is mainly due to the large flow of Yuxi River near point N. The vertical distribution of the water flow directions at points M and N are almost unaffected by the river discharges. This is mainly because the two points selected in the study are in the center of the west lake and the east lake respectively. Through the three-dimensional roaming, it can be found that the river discharges flowing into the lake have a greater impact on the direction of the water flow near the river mouths.

As shown in Fig. 8-11, it is easier to study and compare the lake flow characteristics under different conditions by using the 3DV-HLM method. By operating the mouse, the researchers can analyze the hydrodynamic characteristics of the lake at any position of the lake under different working conditions synchronously, which is more conducive to the lake managers to make the best decision. Through the three-dimensional visualization of data, the results of the hydrodynamic lake model will be more easily accepted by people who have no professional background, which will promote better communication between different stakeholders.

4.4 Future work

This paper mainly studies the integration method of the hydrodynamic lake model and the three-dimensional visualization technology. Although the three-dimensional visualization technology has its unique advantages, in some aspects, the traditional analysis methods also have their advantages. For

example, it is easier to perform quantitative analysis by the traditional analysis methods, and the smaller data volume requires less computer memory.

Follow-up researches can combine the advantages of the traditional analysis methods and the three-dimensional dynamic visualization technology. The virtual reality (VR) technology can also be used so that the lake management and decision-making can be carried out in a more immersive manner. In addition, the three-dimensional visualization technology can be applied to explain more complex water environment processes such as sediment transport, water quality models, algae blooms, etc. The water environment involves a large amount of data, and how to improve the visualization rendering efficiency of the massive data needs further research.

5. Conclusions

The water movement of the lake is a complex problem affected by many factors. In view of the shortcomings of the existing hydrodynamic analysis methods in the data coupling and presentation, this study established a general integrated 3DV-HLM method by combining the hydrodynamic lake model and the three-dimensional dynamic visualization technology. Chaohu Lake in China is taken as an example to analyze the simulated results under 13 working conditions to verify the feasibility of the 3DV-HLM method. The water flow of the lake can be intuitively analyzed and understood from different perspectives by coupling the hydrodynamic lake model and the three-dimensional dynamic visualization technology. The results show that:

(1) Compared with the traditional analysis methods, the 3DV-HLM method is more systematic and efficient in the expression of multi-source heterogeneous information. It can not only show multiple dimensions of simulated water flow results at the same time, but also include the actual three-dimensional terrain, ground features and other information.

(2) The 3DV-HLM method makes it easier to find useful information from huge data and discover potential rules, such as the change rules of the water flows along the water depth, the impact of actual topography and ground features on the water flows, etc.

(3) The vivid and intuitive visualization of model results by the 3DV-HLM method is closer to the real three-dimensional environment, which can enhance the understanding of the hydrodynamic characteristics of the lake by the lake managers and promote better communication between different stakeholders.

Declarations

Funding

Major Science and Technology Program for Water Pollution Control and Treatment (Grant No. 2018ZX07208006)

Major Science and Technology Program for Water Pollution Control and Treatment (Grant No. 2017ZX07603001)

Conflicts of interest/Competing interests

The authors declare that they have no known competing financial interests or personal relationships that could have appeared to influence the work reported in this paper.

Availability of data and material

Not applicable

Code availability

Delft3D: https://oss.deltares.nl/web/delft3d/source-code

Authors' contributions

Xianyong Gu: Conceptualization, Methodology, Software, Investigation, Writing - original draft, Writing - review & editing, Visualization.

Zhenliang Liao: Conceptualization, Writing - review & editing, Resources, Supervision, Project administration, Funding acquisition.

Guozheng Zhi: Methodology, Writing - review & editing.

Wenchong Tian: Software, Writing - review & editing.

Jiaqiang Xie: Writing - original draft, Writing - review & editing.

References

Cao J, Peng H (2009) Two-dimensional flow-pollutant model and its application to shallow lake in Suzhou City. IEEE Int Semin Bus Inf Manage 2008: 105-108. https://doi.org/10.1109/ISBIM.2008.126

Kolditz O, Rink K, Nixdorf E, Fischer T, Bilke L, Naumov D, Liao Z, Yue T (2019) Environmental information systems: paving the path for digitally facilitated water management (Water 4.0). Eng 5(5): 828-832. https://doi.org/10.1016/j.eng.2019.08.002

Li J, Tooth S, Zhang K, Zhao Y (2021) Visualisation of flooding along an unvegetated, ephemeral river using Google Earth Engine: Implications for assessment of channel-floodplain dynamics in a time of rapid environmental change. J Environ Manage 278: 111559. https://doi.org/10.1016/j.jenvman.2020.111559

Li Z, Sun J, Zhang J (2012) A new approach of building 3D visualization framework for multimodal medical images display and computed assisted diagnosis. Proc SPIE 8425:206. https://doi.org/10.1117/12.911052

Nutz A, Schuster M, Ghienne J F, Roquin C, Hay M B, Rétif F, Certain R, Robin N, Raynal O, Cousineau PA (2015) Wind-driven bottom currents and related sedimentary bodies in Lake Saint-Jean (Québec, Canada). Geol Soc Am Bull. 9:1194-1208. http://doi.org/10.1130/b31145.1

Pang C, Wang F, Wu S, Lai X (2015) Impact of submerged herbaceous vegetation on wind-induced current in shallow water. Ecol Eng 81: 387-394. https://doi.org/10.1016/j.ecoleng.2015.04.021

Qi L, Huang J, Gao J, Cui Z (2019) Modelling the impacts of bathymetric changes on water level in China's largest freshwater lake. Water 11(7): 1469. https://doi.org/10.3390/w11071469

Ren L, Nash S, Hartnett M (2015) Observation and modeling of tide- and wind-induced surface currents in Galway Bay. Water Sci Eng 8(4): 345-352. https://doi.org/10.1016/j.wse.2015.12.001

Robinson J, Buda A, Collick A (2020) Electrical monitoring of saline tracers to reveal subsurface flow pathways in a flat ditch-drained field. J Hydrol 586:124862. https://doi.org/10.1016/j.jhydrol.2020.124862

Rodriguezgonzalvez P, Rodriguezmartin M, Fradejas B A, Alvearordenes I (2018) 3D visualization techniques in health science learning: application case of thermographic images to blood flow monitoring. Proc 6th Int Conf Technol Ecosyst Enhancing Multiculturality 10: 373-380. https://doi.org/10.1145/3284179.3284243

Saravanavel J, Ramasamy S M (2020) GIS based 3D visualization of subsurface geology and mapping of probable hydrocarbon locales, part of Cauvery Basin, India. J Earth Syst Sci 129(1): 36. https://doi.org/10.5194/isprsarchives-XL-8-469-2014

Tame C, Cundy A B, Royse K R, Smith M, Moles N R (2013) Three-dimensional geological modelling of anthropogenic deposits at small urban sites: A case study from Sheepcote Valley, Brighton, UK. J Environ Manage 129(15):628-634. https://doi.org/10.1016/j.jenvman.2013.08.030

Wang C, Fan X, Wang P, Hou J (2016) Flow characteristics of the wind-driven current with submerged and emergent flexible vegetations in shallow lakes. J Hydrodyn 28(5):746-756. https://doi.org/10.1016/S1001-6058(16)60677-7

Wang J, Weng S, Wu S, Hu X, Yang X (2019) The visualization of flow field around circular cylinders by fluent standard k–ε turbulence model. IOP conference series Earth Environ Sci 344: 12134. https://doi.org/10.1088/1755-1315/344/1/012134

Wang Y, Huynh G, Williamson C (2013) Integration of google maps/earth with microscale meteorology models and data visualization. Comput Geosci 61: 23-31. http://dx.doi.org/10.1016/j.cageo.2013.07.016

Wang Z, Wang K, Liu K, Cheng L, Ye A (2019) Interactions between lake-level fluctuations and waterlogging disasters around a large-scale shallow lake: an empirical analysis from China. Water 11(2): 318. http://dx.doi.org/10.3390/w11020318

Wu J, Tsanis I K (1995) Numerical study of wind-induced water currents. J Hydraul Eng 121(5): 388-395. http://dx.doi.org/10.1061/(ASCE)0733-9429(1995)121:5(388)

Wurjanto A, Ajiwibowo H (2019) Modelling the spatial concentration distribution of environmental parameters and total suspended sediment in Diatas lake, western Sumatra, Indonesia. Int J Geomate 17(63): 288-296. http://dx.doi.org/10.21660/2019.63.11727

Yadav A, Zhang N (2020) Hydraulic simulation for calcasieu lake area with small rivers using an immersed boundary method. J Fluids Eng 142(2): 021503. http://dx.doi.org/10.1115/AJKFluids2019-4675

Ying W, Liu A, Zhu Y, Li M, Liu B (2018) The research on Ntot pollutant dispersion provoked by wind-driven currents. IOP Conf Ser: Earth Environ Sci 153:062068. http://dx.doi.org/10.1088/1755-1315/153/6/062068

Zhang H, Culver D A, Boegman L (2008) A two-dimensional ecological model of lake Erie: Application to estimate dreissenid impacts on large lake plankton populations. Ecol Modell 214(2-4):219-241. http://dx.doi.org/10.1016/j.ecolmodel.2008.02.005

Zhang N, Han X, Wang W (2019) A comprehensive hydrodynamics-salinity-pH model for analyzing the effects of freshwater withdrawals in Calcasieu Lake and surrounding water systems. J Fluids Eng 141(5): 051103. http://dx.doi.org/10.1115/1.4041455

Zhang Y, Lai X, Zhang L, Song K, Yao X, Gu L, Pang C (2020) The influence of aquatic vegetation on flow structure and sediment deposition: A field study in Dongting Lake, China. J Hydrol 584: 124644. https://doi.org/10.1016/j.jhydrol.2020.124644

Zhang Z, Huang C, Guo F, Song Z, Hu D (2019) A new technology for suspended sediment simulation in Lake Taihu, China: Combination of hydrodynamic modeling and remote sensing. J Limnol 78(1): 121-134. https://doi.org/10.4081/jlimnol.2019.1813

Zhi G, Liao Z, Tian W, Wang X, Chen J (2019) A 3D dynamic visualization method coupled with an urban drainage model. J Hydrol 577: 123988. https://doi.org/10.1016/j.jhydrol.2019.123988

Zhao G, Gao X, Zhang C, Sang G (2020) The effects of turbulence on phytoplankton and implications for energy transfer with an integrated water quality-ecosystem model in a shallow lake. J Environ Manage 256: 109954. https://doi.org/10.1016/j.jenvman.2019.109954

Figure Captions

Fig.1 The theoretical framework of the research

Fig.2 Location of Chaohu Lake

Fig.3 Principle of the data interface

Fig.4 Schematic diagram of the three-dimensional terrain construction

Fig.5 The color band

Fig.6 The flow arrow coordinate system

Fig.7 The flow fields at different simulating times under the typical operating condition (a:1h; b:4h; c:12h; d:72h)

Fig.8 The flow fields after stabilization under different water levels (a: scheme 1; b: scheme 2; c: scheme 3; d: scheme 4)

Fig.9 The flow fields after stabilization under different wind directions (a: scheme 2; b: scheme 5; c: scheme 6; d: scheme 7)

Fig.10 The flow fields after stabilization under different wind speeds (a: scheme 8; b: scheme 2; c: scheme 9; d: scheme 10)

Fig.11 The water flow after stabilization under different river flows into the lake (a: scheme 11; b: scheme 12; c: scheme 13)

Fig. 12 Comparison of the traditional analysis method and the 3DV-HLM method (a: surface layer of the flow field; b: middle layer of the flow field; c: bottom layer of the flow field; d: vertical distribution of velocity magnitude and direction at point P; e: three-dimensional flow field; f: enlarged view of the flow field; g: vertical distribution of the velocity at point P)

Figures

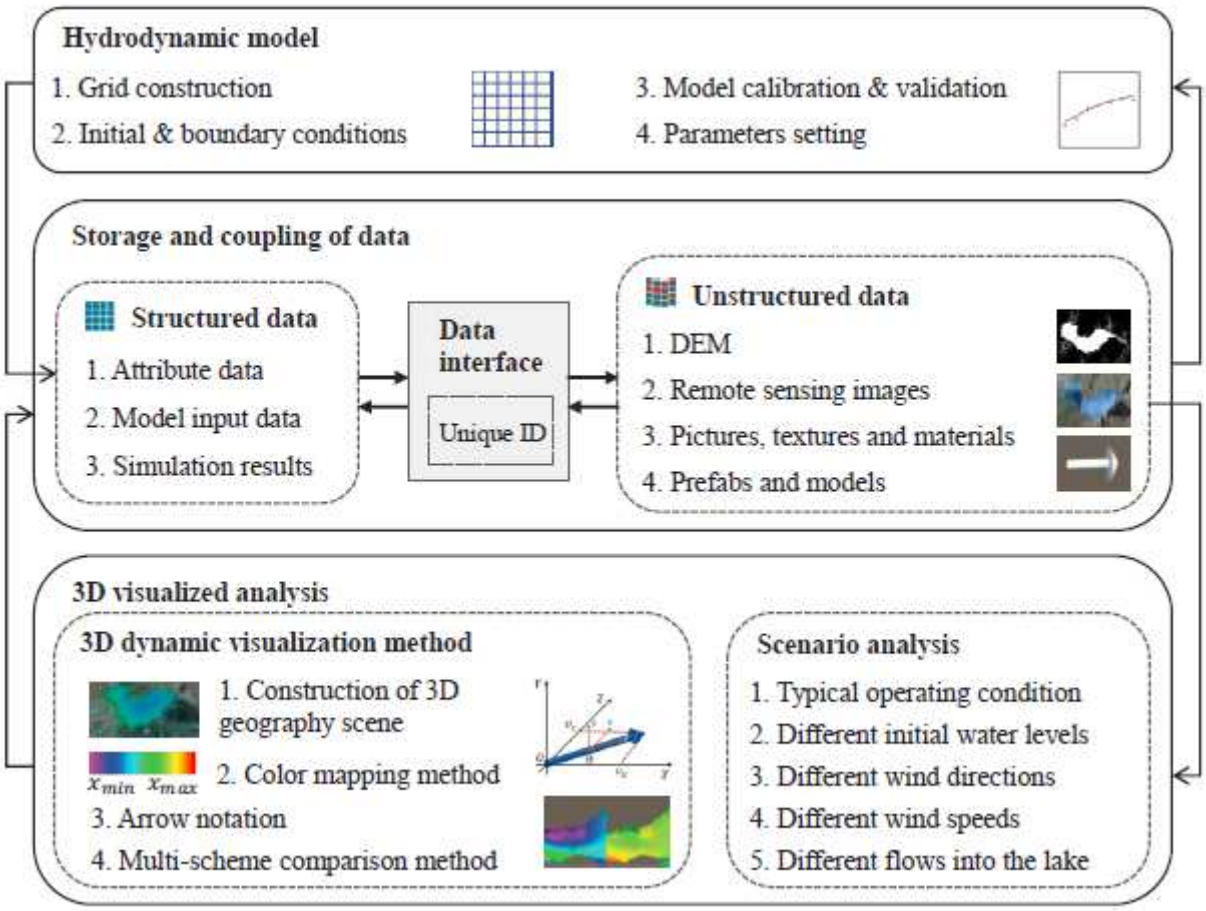

Figure 1

The theoretical framework of the research

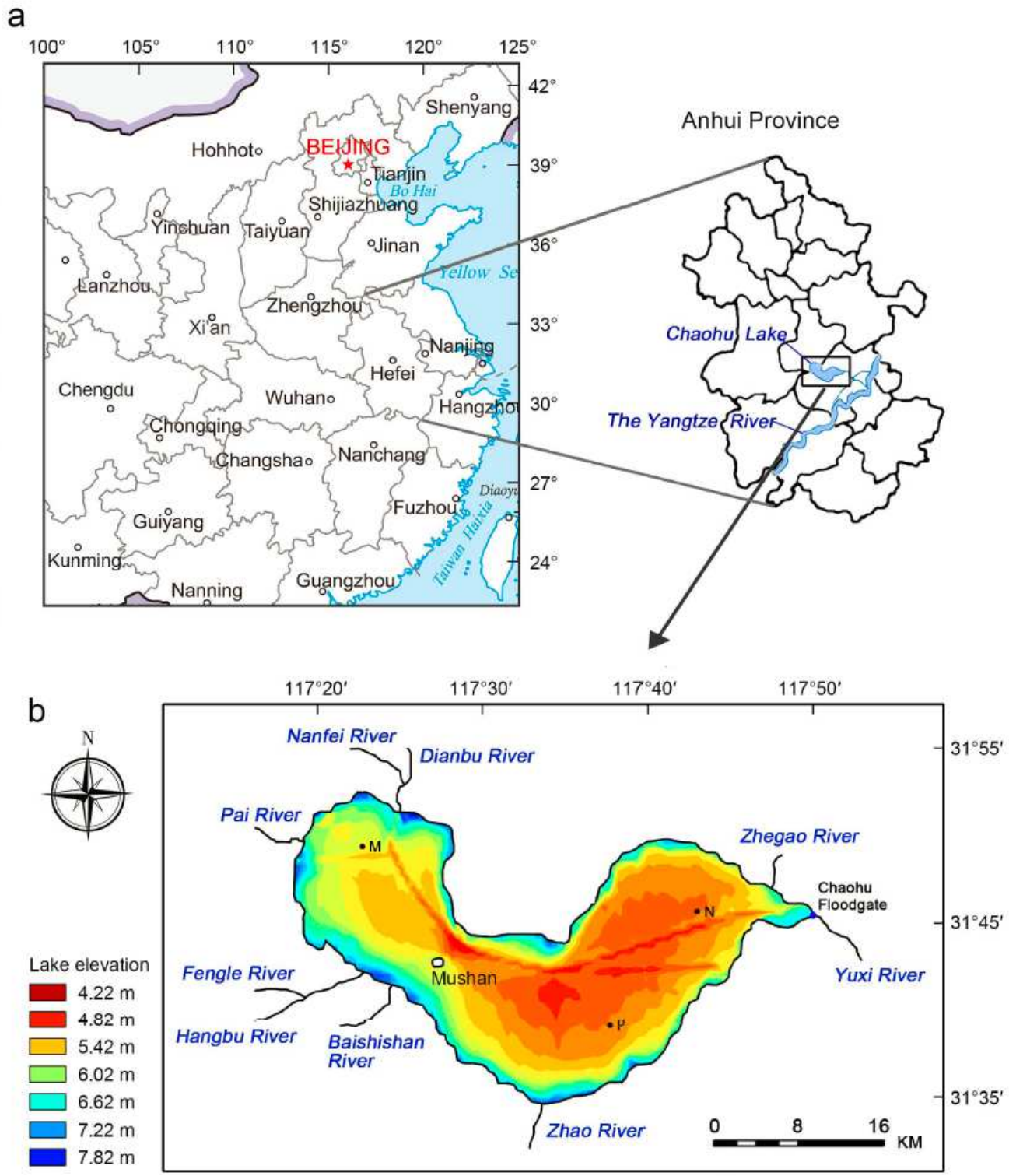

Figure 2

Location of Chaohu Lake

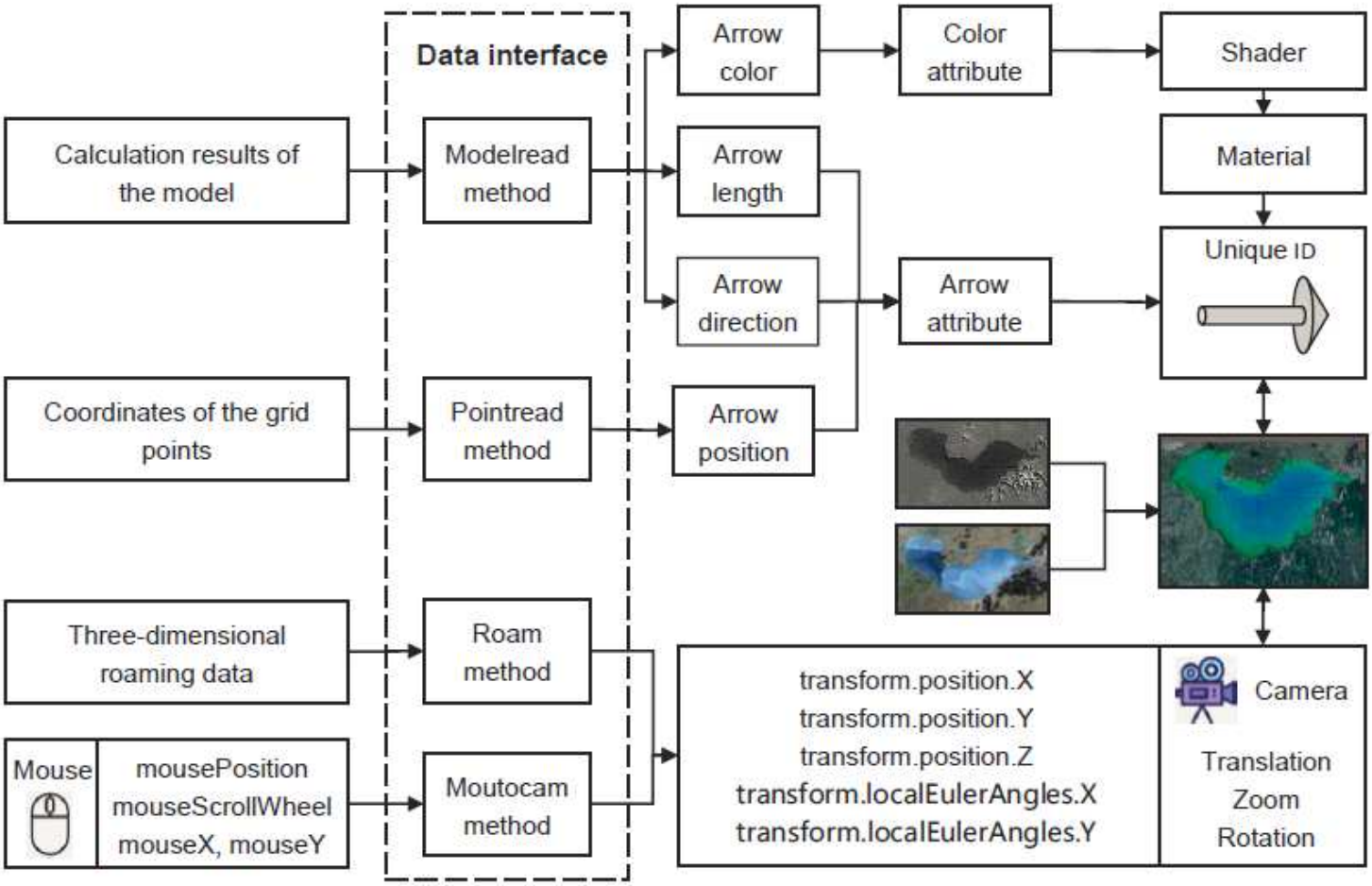

Figure 3

Principle of the data interface

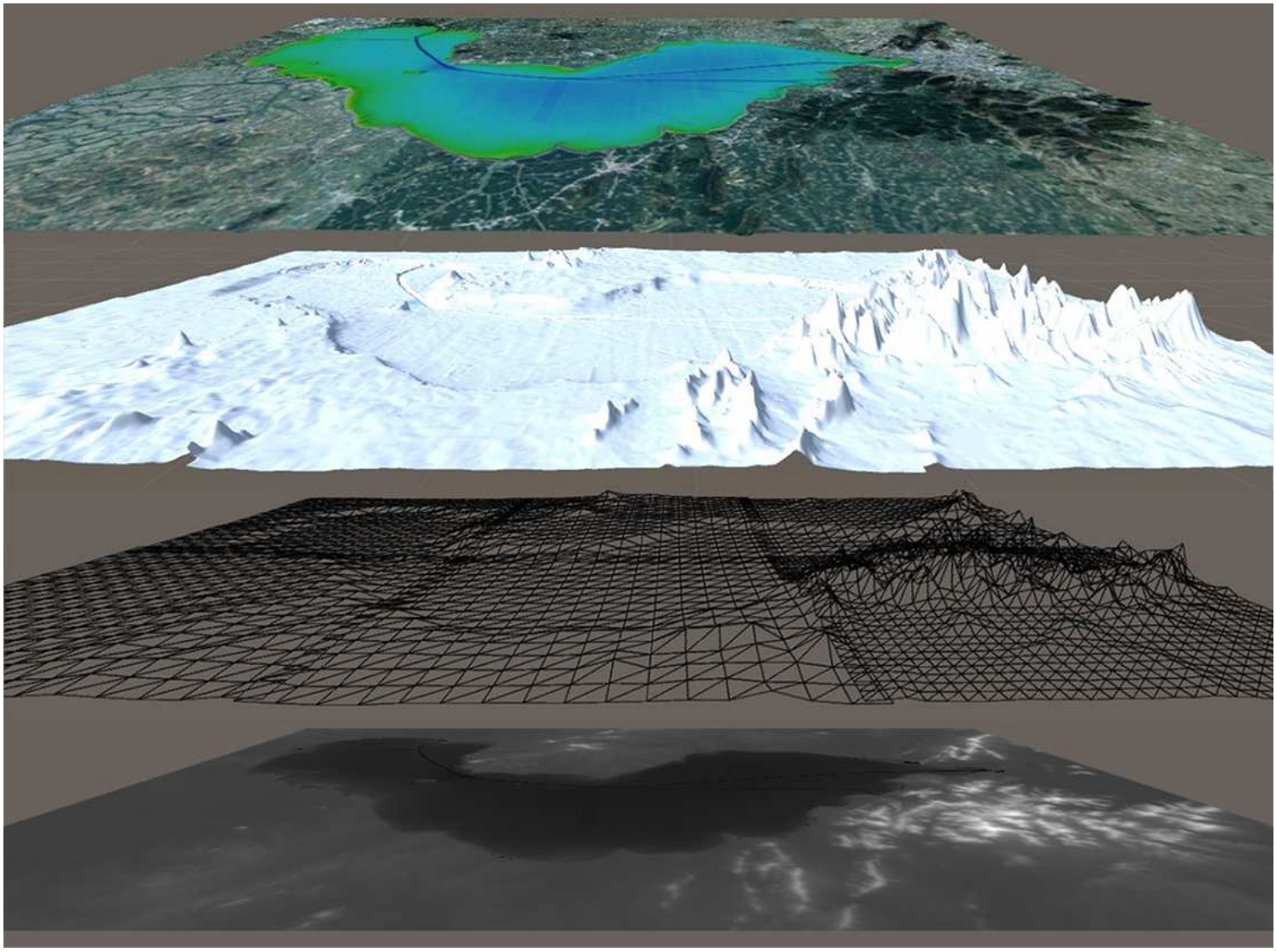

Figure 4

Schematic diagram of the three-dimensional terrain construction

Figure 5

The color band

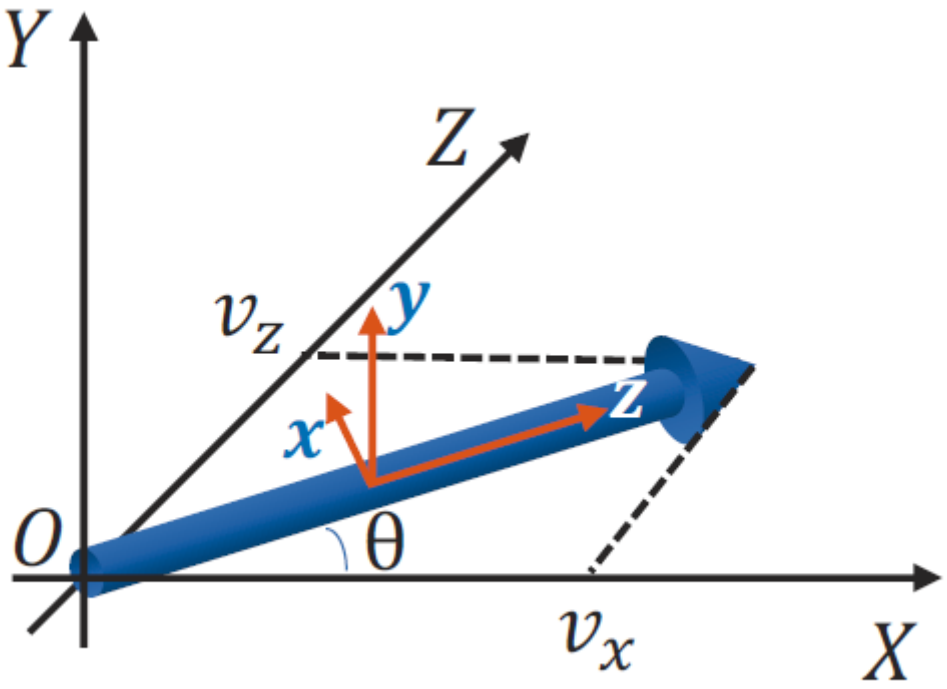

Figure 6

The flow arrow coordinate system

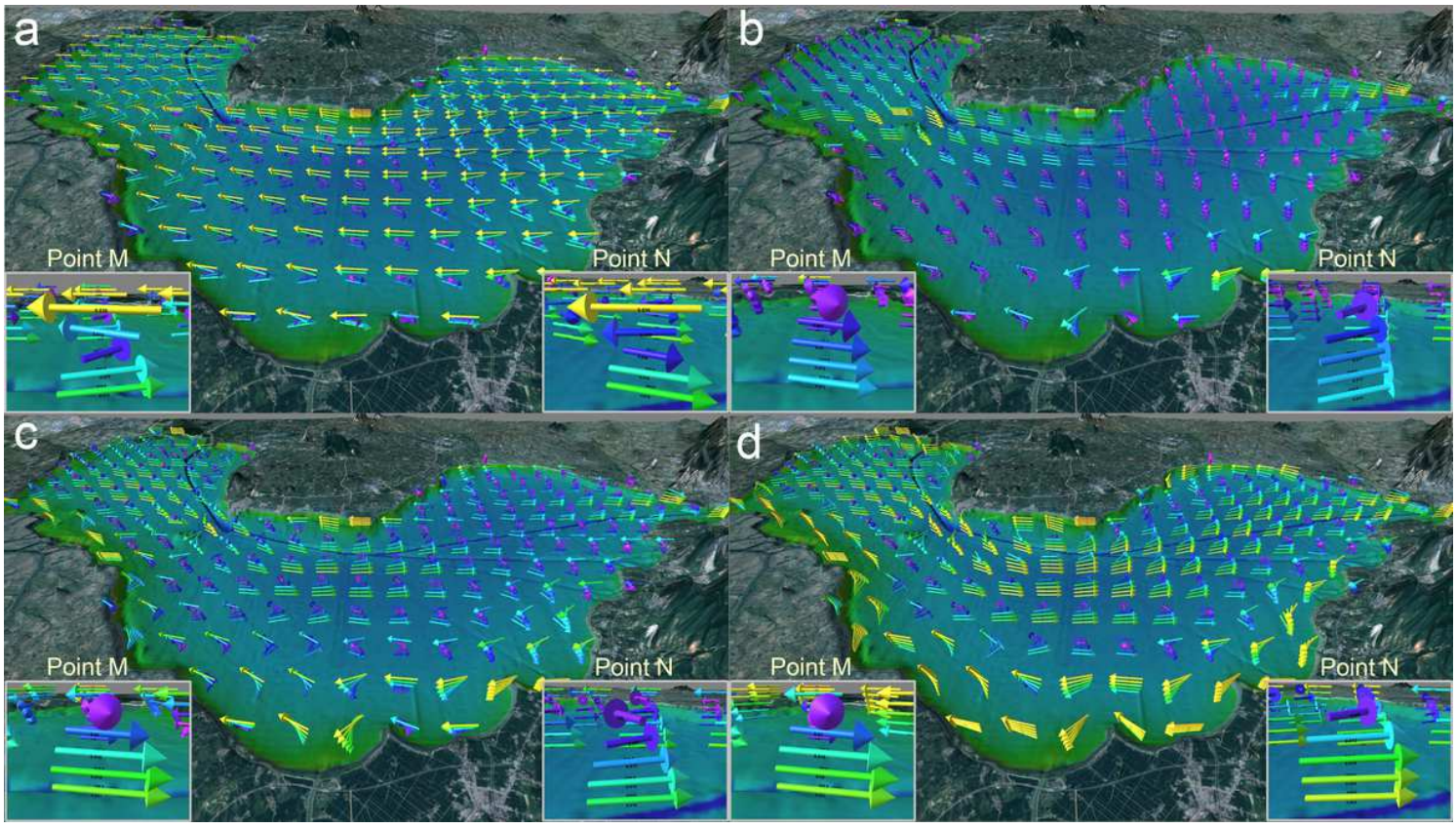

Figure 7

The flow fields at different simulating times under the typical operating condition (a:1h; b:4h; c:12h; d:72h)

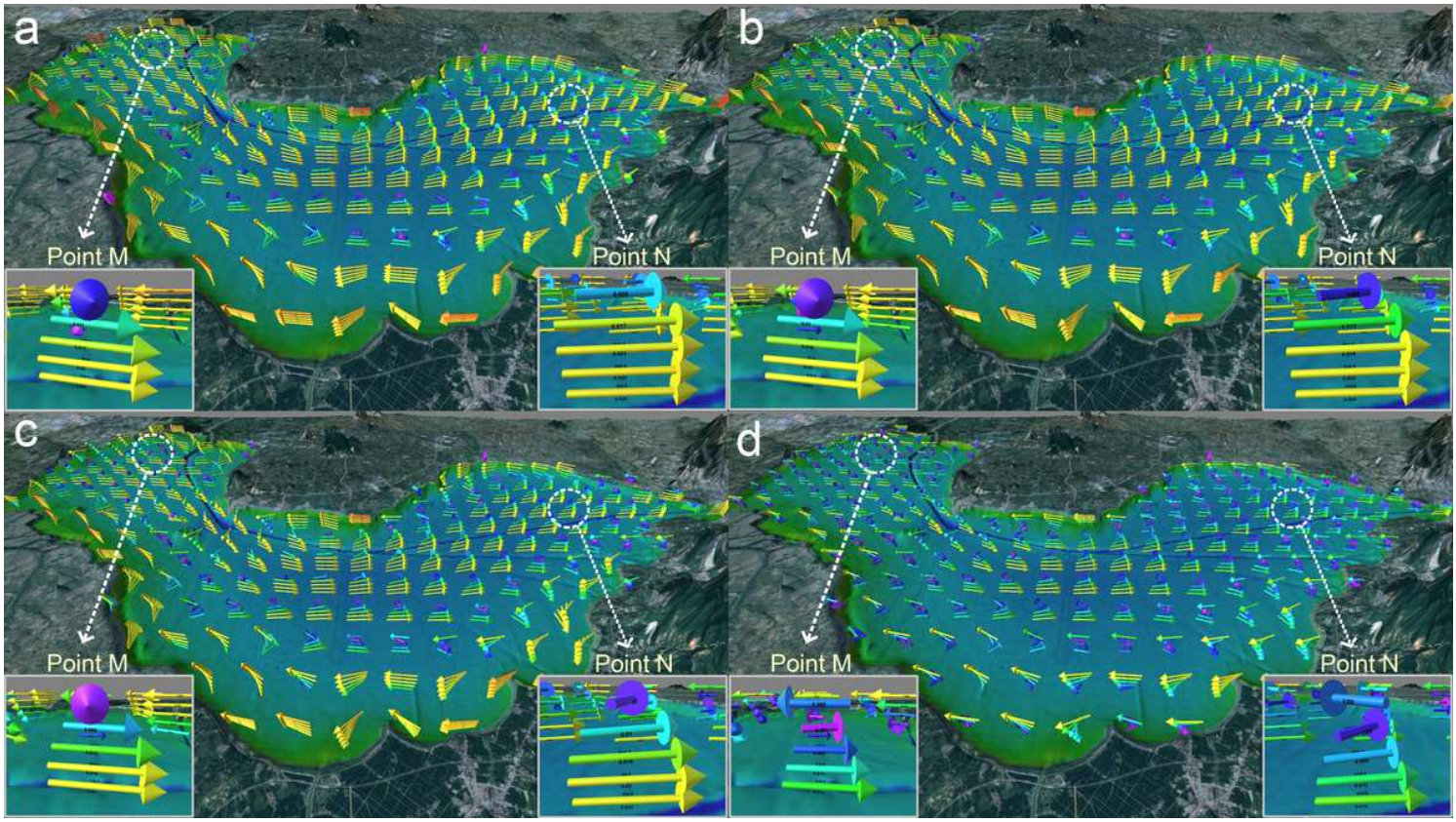

Figure 8

The flow fields after stabilization under different water levels (a: scheme 1; b: scheme 2; c: scheme 3; d: scheme 4)

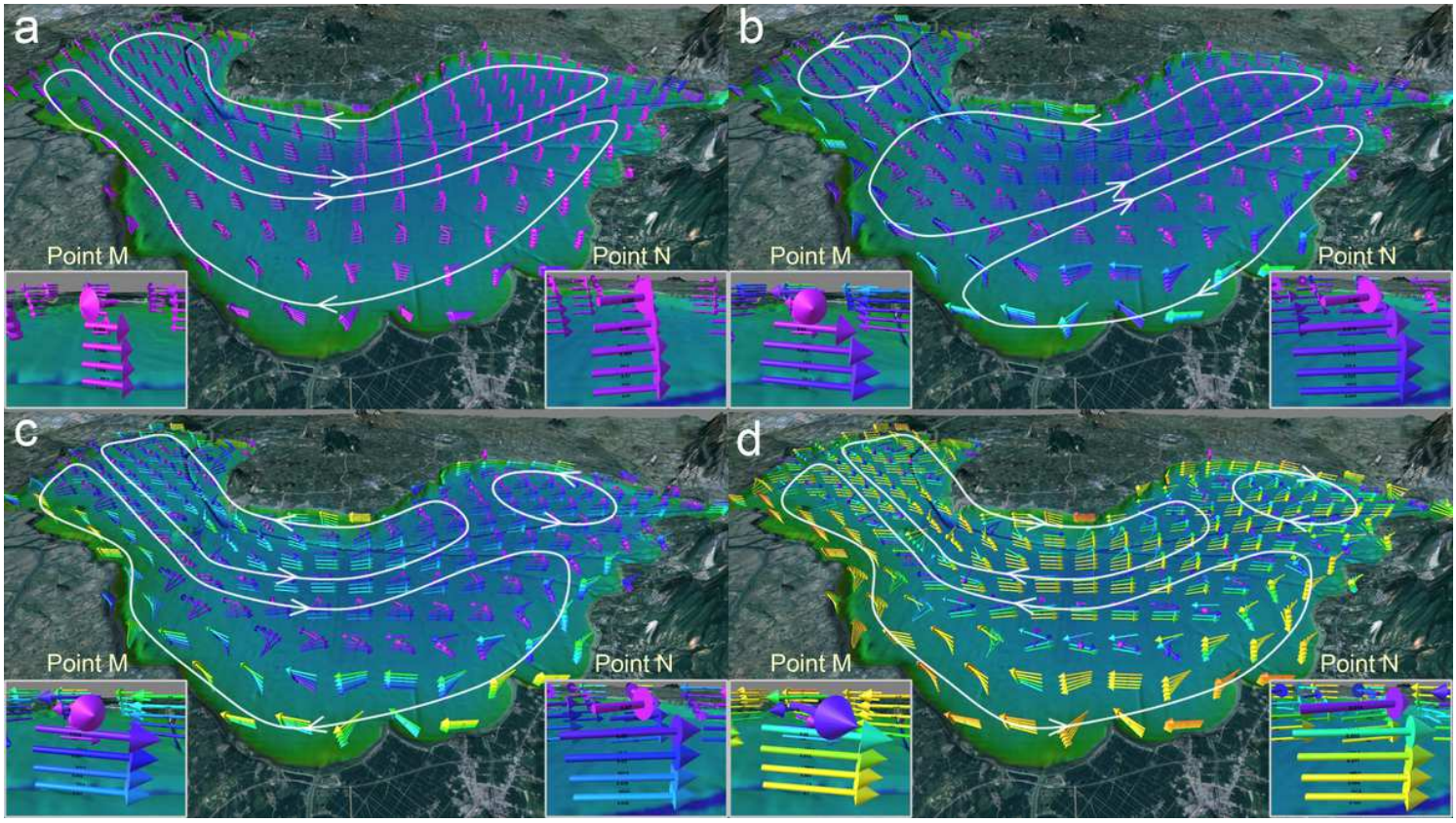

Figure 9

The flow fields after stabilization under different wind directions (a: scheme 2; b: scheme 5; c: scheme 6; d: scheme 7)

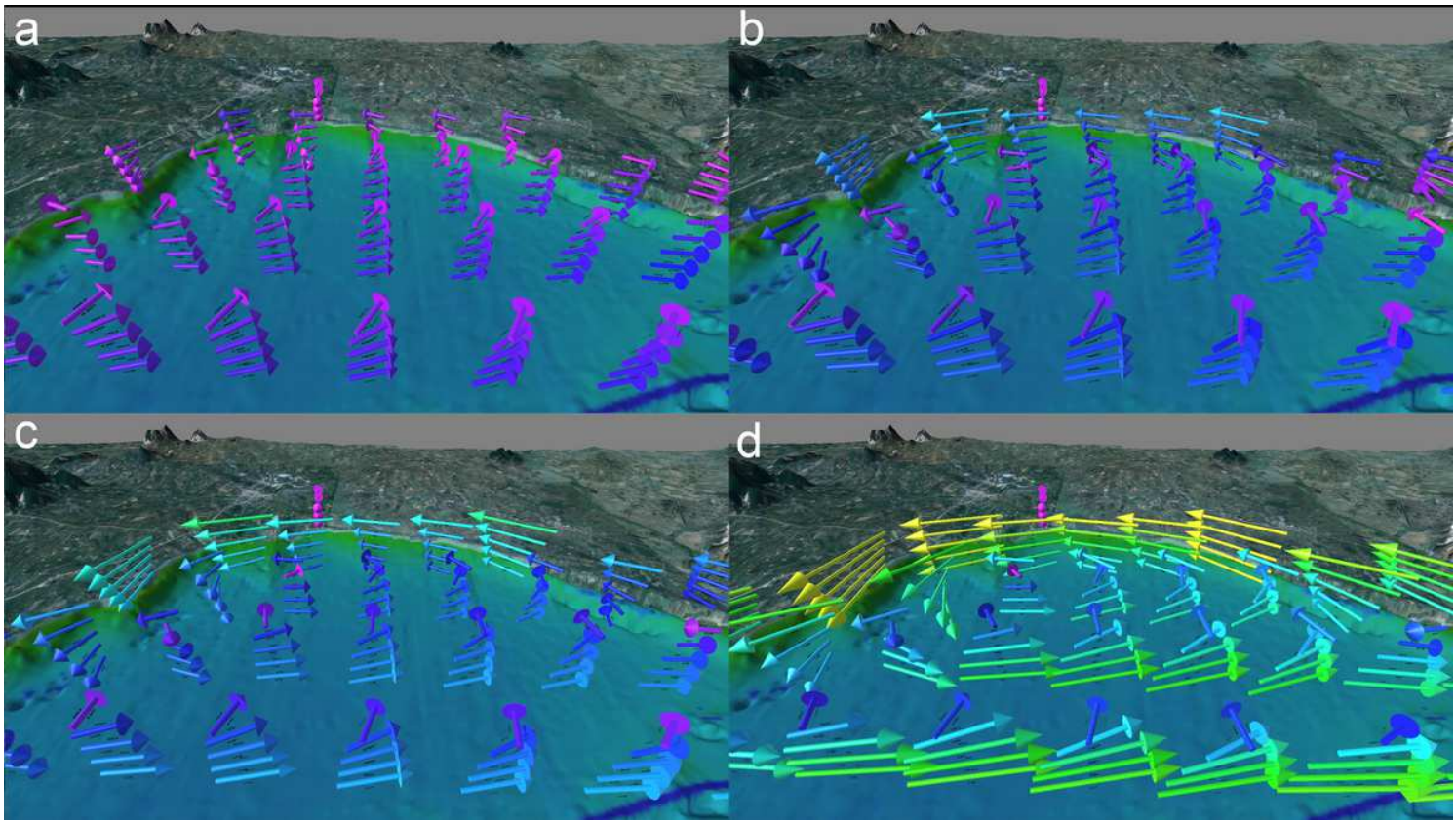

Figure 10

The flow fields after stabilization under different wind speeds (a: scheme 8; b: scheme 2; c: scheme 9; d: scheme 10)

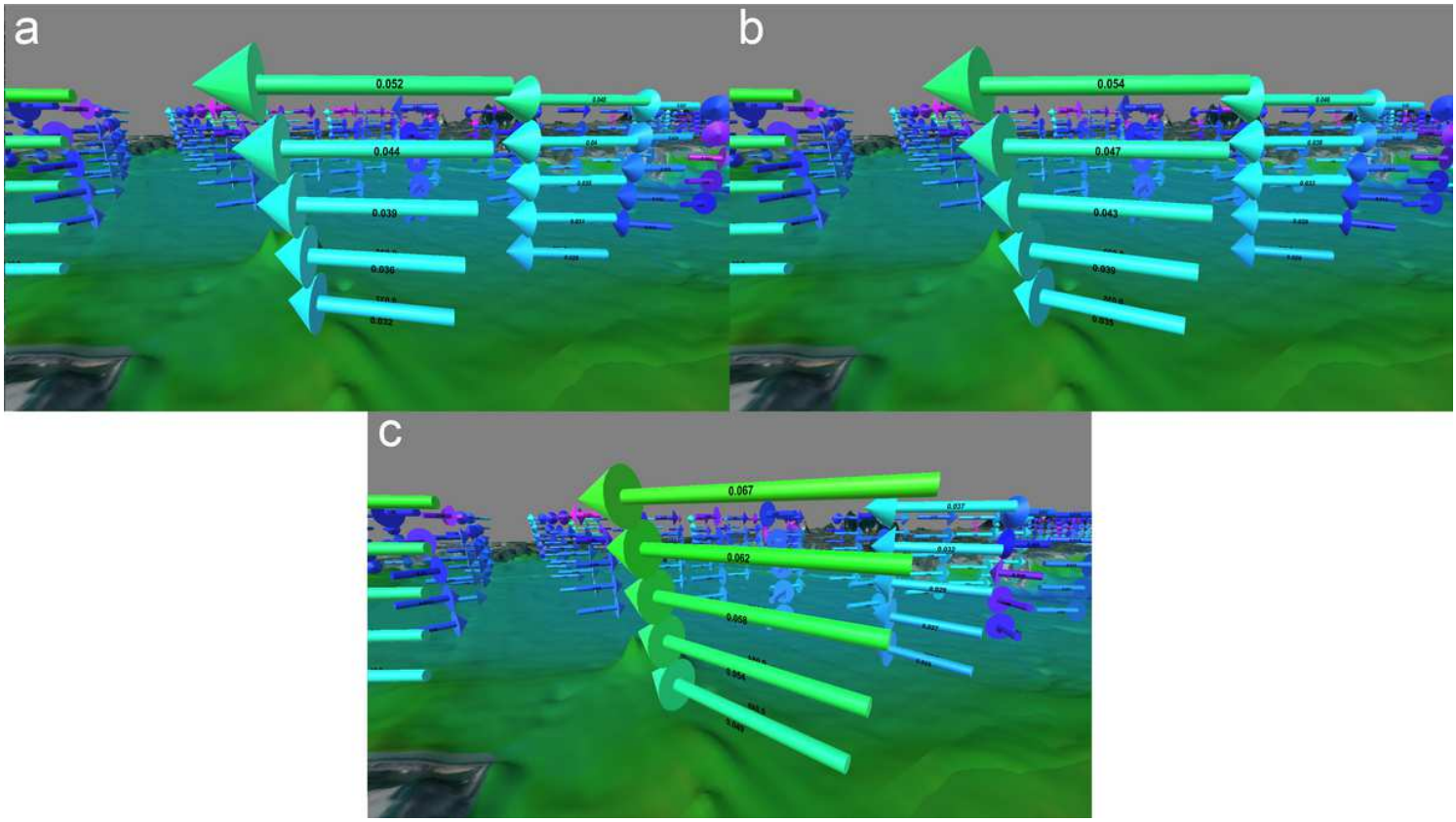

Figure 11

The water flow after stabilization under different river flows into the lake (a: scheme 11; b: scheme 12; c: scheme 13)

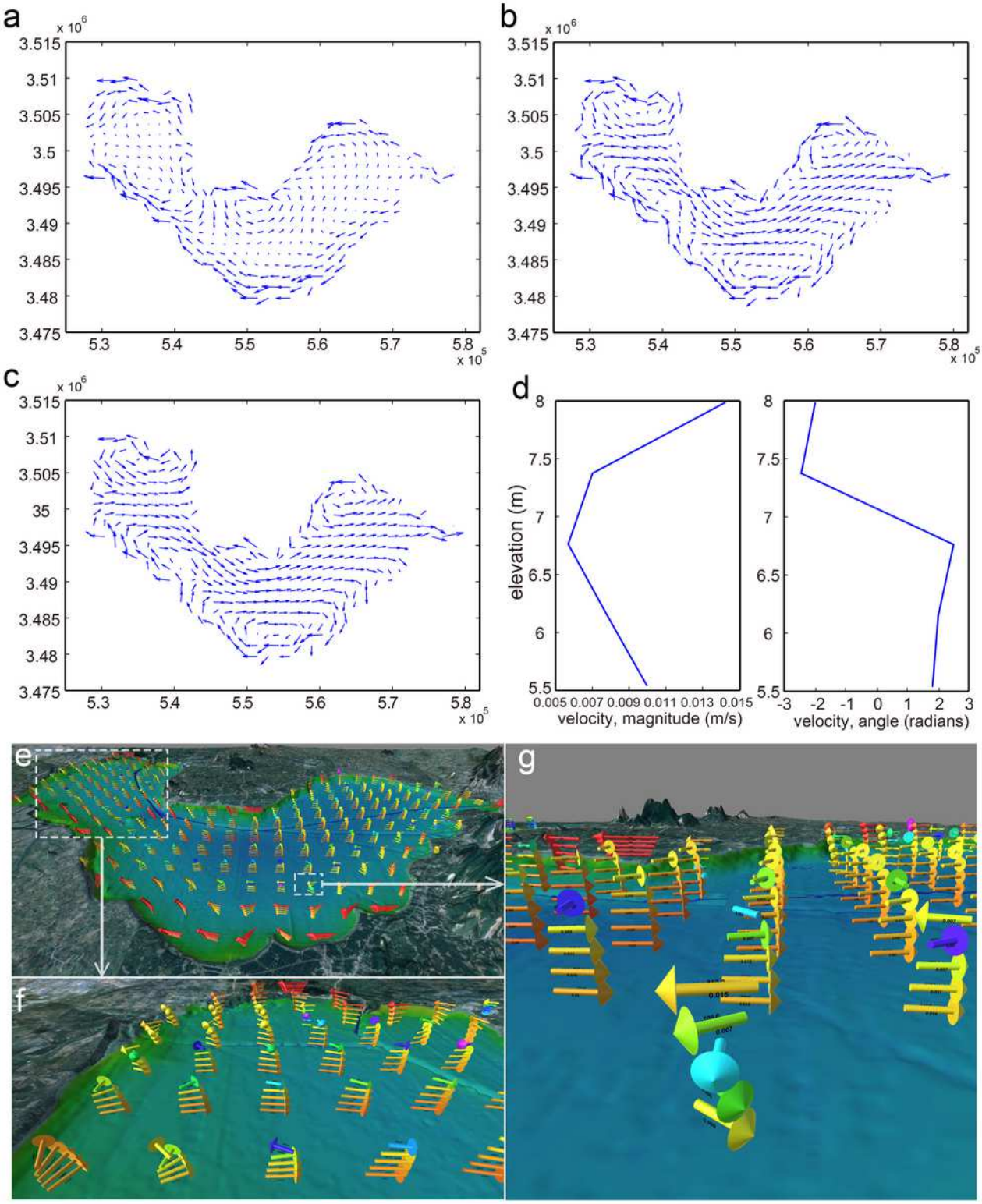

Figure 12

Comparison of the traditional analysis method and the 3DV-HLM method (a: surface layer of the flow field; b: middle layer of the flow field; c: bottom layer of the flow field; d: vertical distribution of velocity magnitude and direction at point P; e: three-dimensional flow field; f: enlarged view of the flow field; g: vertical distribution of the velocity at point P)